Soft Materials
Publication details, including instructions for authors and subscription information:
http://www.tandfonline.com/loi/lsfm20

Aggregate Structural Transitions Noticed for the Didodecyldimetilammonium Bromide-Sodium Dehydrocholate Catanionic Mixed System at Low Concentration

Marcos D. Fernández-Leyes [a], Paula V. Messina [a], Noemí Andreucetti [a], Carina Luengo [a] & Pablo C. Schulz [a]

[a] Departamento de Química, CONICET-INQUISUR, Universidad Nacional del Sur, Bahía Blanca, Argentina

Accepted author version posted online: 24 Oct 2011.Published online: 04 Jan 2013.

To cite this article: Marcos D. Fernández-Leyes , Paula V. Messina , Noemí Andreucetti , Carina Luengo & Pablo C. Schulz (2013): Aggregate Structural Transitions Noticed for the Didodecyldimetilammonium Bromide-Sodium Dehydrocholate Catanionic Mixed System at Low Concentration, Soft Materials, 11:2, 204-214

To link to this article: http://dx.doi.org/10.1080/1539445X.2012.617642

Soft Materials (2013) **11**, 204–214

ISSN: 1539-445X print / 1539-4468 online
DOI: 10.1080/1539445X.2012.617642

Taylor & Francis
Taylor & Francis Group

Aggregate Structural Transitions Noticed for the Didodecyldimetilammonium Bromide-Sodium Dehydrocholate Catanionic Mixed System at Low Concentration

MARCOS D. FERNÁNDEZ-LEYES, PAULA V. MESSINA*, NOEMÍ ANDREUCETTI, CARINA LUENGO, and PABLO C. SCHULZ

Departamento de Química, CONICET-INQUISUR, Universidad Nacional del Sur, Bahía Blanca, Argentina

Received 04 February 2010, Accepted 25 January 2011

The phase behavior for the very diluted DDAB-NaDHC-water system was investigated at 25°C. Fluorescence, conductivity, and surface tension experiments were carried out to determine the cac values. Comparison between experimental and calculated values shows the suitability of the regular theory to predict the critical aggregation concentrations for the tested systems. The interaction between both amphiphiles inside aggregates is not ideal, showing a large synergism. Such fact is reflected by the activity of coefficients values. The aggregates are mainly comprised by DDAB (18–30 % mol NaDHC) regardless of the NaDHC solution molar fraction; these molecules act as a good solvent of bile salt type molecule. Nevertheless, the gradual inclusion of NaDHC molecules inside DDAB bilayers leads to structural transformations. These facts are supposed to be due the combination of two effects: (i) the reduction of head groups hydration and (ii) the increment of chain repulsion.

Keywords: Aggregate transitions, DDAB, NaDHC, Regular Solution Theory, Vesicles

Introduction

Unlike conventional surfactant molecules, bile salts (BSs) possess a rigid steroid backbone having polar hydroxyl groups on the concave α-face and methyl groups on the convex one. This arrangement creates a unique facial amphiphilicity for this class of molecules, causing aggregation in water different from that of conventional amphiphiles. Because of their biological relevance, BSs have been studied throughout the years in mixed amphiphilic systems, with both natural (1–3) and synthetic surfactants (4, 5) as well as with cholesterol (6). A variety of liquid crystalline structures is present in these strongly associative mixtures. A particular type of mixed system is the so-called catanionic surfactant mixture, a mixture of an anionic and a cationic surfactant where their respective counterions are also present. These mixtures have important technical applications, like those related with enhanced interfacial performance or control rheological properties of materials.

In this work, the phase behavior and the aggregate structure analysis for the sodium dehydrocholate (NaDHC)-didodecyldimethylammonium bromide (DDAB) system, at low concentrations, are presented. The DDAB molecule has low water solubility and its packing parameter, close to unity, dictates a preference to assemble into bilayer-based structures (7, 8). The sodium dehydrocholate (NaDHC) molecule has three carbonyl groups at positions 3, 7, and 12 of the steroid backbone. We determined that it presents a stepwise aggregation to give rise to micelles (9, 10). Mixtures of micelle-forming with vesicle-forming surfactants yield formation of either micelle or vesicle structures as well as intermediate structures or phase separation depending on the surfactant architecture and concentration (11, 12). BSs can thus be used as additive (co-surfactant) to stabilize or destabilize vesicle structures, as well as to modify their properties. Both vesicles and micelles are important in many applications and the capability of forming either vesicles or micelles from an aqueous mixture of surfactants, by varying only the surfactant compositions, is a very promising research field.

The aim of this study is, on one hand, to obtain precise information of critical concentrations at which the aggregation of the NaDHC- DDAB aqueous mixture occurs and to evaluate the aggregates structure transitions. On the other hand, we investigate the applicability of the different theoretical models (traditionally used with classical surfactants) on mixed micellization. For this purpose, this paper is organized as follow; initially we report fluorescence intensities ratios of the first and third pyrene emission spectra (I_1/I_3) as a function of the total surfactant concentration. Critical concentrations are obtained from such plots and confirmed by surface tension and conductivity measurements. Following, the aggregate structure is evaluated from TEM microphotographs, dynamic light scattering, and Zeta potential measurements. Finally, the existence of synergism and the interaction parameters based on the different theoretical approximations are investigated.

*Address correspondence to: Paula V. Messina, Departamento de Química, CONICET-INQUISUR, Universidad Nacional del Sur (8000) Bahía Blanca, Argentina. Email: pmessina@uns.edu.ar

Experimental

Materials

Dehydrocholic acid (HDHC) was obtained from Dr. Theodor Schuchardt (Munich) and was of analytical grade. Didodecyldimethylammonium bromide (DDAB) was obtained from Aldrich, 99%, and used as purchased. Pyrene (Sigma-Aldrich, 99%) was used as fluorescence probe.

Solutions

Dehydrocholic acid sodium salt (NaDHC) solution was prepared by weighing a quantity of HDHC and by dissolution in an appropriate amount of concentrated NaOH.

Stock NaDHC and DDAB solutions (0.1 mol dm^{-3}) were prepared and diluted as required for each experiment. The appropriate amounts of NaDHC and DDAB stock solutions were mixed to obtain the different NaDHC-DDAB mixture solutions.

All surfactants and fluorescence probe solution were prepared using double-distilled water.

Methods

Experimental Techniques

Fluorescence spectra of pyrene were obtained with a SHIMADZU RF-5301PC Spectrofluorophotometer. All samples were prepared with saturated solutions of pyrene (3×10^{-7} mol dm^{-3}). Measurements were performed at 298 ± 2 K and the fluorescence intensities ratios (I_1/I_3) of the first (I_1, 373 nm) and third (I_3, 384 nm) peaks from the short wavelength in the spectra of pyrene were obtained with excitation at 335 nm. The excitation and emission slit widths were set to be 5 and 1.5 nm, respectively.

Solutions of (0.4–10) mM concentrations for all mixed proportions were treated with a solution of uranyl acetate following a staining technique to study the aggregates by transmission electron microscopy as described in literature (13, 14).

Conductivity measurements were performed with an immersion cell and an automatic conductimeter, namely, Antares II from Instrumentalia. Surface tension was measured with a ring tensiometer from Krüss. All determinations were performed by titration of 50 mL of a stock solution (0.1 mol dm^{-3}) of each pure surfactant and their mixtures with water at 25.0 ± 0.1°C.

A Malvern Zeta Sizer Nano (ZS90) with a He-Ne laser (λ = 633nm) was used for dynamic light scattering (DLS) and Zeta potential (ζ) measurements. For DLS determinations, the scattering angle was 90° and a disposable polystyrene cell was used. The results were corrected for medium viscosity effect using 1.330 as the refractive index (RI). Malvern's software provides a mean diameter weighed by the scattered intensity (z-averaged hydrodynamic mean diameter, *D*). The polydispersity given by the apparatus is equivalent to the variance of a long-normal distribution. All measurements were achieved in triplicate. Experimental errors were estimated to be ±1 and ±5% for diameters lower and larger than 200 nm, respectively. Zeta potentials of different NaDHC/DDAB systems were made using a clear disposable zeta cell by taking the average of five measurements at the stationary level. The zeta potential was calculated from electrophoretic mobilities (μ_E), using the Henry equation (15):

$$\zeta = \frac{3\mu_E \eta}{2\varepsilon_0 \varepsilon_r} \times \frac{1}{f(ka)} \tag{1}$$

where ε_0 is the permittivity of vacuum, ε_r, and η are the relative permittivity and viscosity of water, respectively, *a* the particle radii and *k* the Debye length. The function $f(ka)$ depends on the particle shape and for our systems were determined by:

$$f(ka) = \frac{2}{3} - \frac{9}{2ka} + \frac{75}{2k^2a^2} - \frac{330}{k^3a^3} \tag{2}$$

valid for $ka > 1$. Equation fitting were done from non-linear procedures using ORIGIN® computer package (release 7.0).

Theoretical Methods

Micellar behavior was analyzed by the employ of theoretical models for mixed micellar systems based on the pseudo-phase separation approach. Such models assume that the mixed micelles can be treated as a phase separated from monomers in the solution. The simplified treatment and modeling of such theoretical models may be one main reason of their use by most researchers in the field (16).

Clint's Model (17). The relationship between the critical micellar concentration of the mixed system and that of the *i* pure components, cmc_M, and cmc_i, respectively, and the total molar fraction in the surfactant mixture without considering the solvent α_i, is given by the expression:

$$\frac{1}{cmc_M} = \sum_i \frac{\alpha_i}{cmc_i} \tag{3}$$

Although Clint's model for the ideal mixed micelle solutions is appropriate only for very few systems, this development has been used often as a way of analyzing the deviation of a mixed system from the ideal behavior (18).

Rubingh's Model (19). It is based on a regular solution approach to the treatment of non-ideal mixing and due to its simplicity; it has been the main model used, even after the development of more complex models. The non-ideality is introduced with the inclusion of the activity coefficients γ_i, into the relationship between the critical micellar concentration of the mixed system (cmc_M) and of the *i* pure components (cmc_i):

$$\frac{1}{cmc_M} = \sum_i \frac{\alpha_i}{\gamma_i\, cmc_i} \tag{4}$$

For a binary solution, for example, according to this model we have:

$$\gamma_i = \exp\left[\beta_M (1 - X_i)^2\right] = \exp\left[\beta_M \left(X_j\right)^2\right] \tag{5}$$

$$\gamma_j = \exp\left[\beta_M (X_i)^2\right] \tag{6}$$

Here, X_i is the molar fraction of the ith surfactant in the micelle and the β_M parameter (in kT units, where k is the Boltzmann constant and T the absolute temperature) can be interpreted in terms of an energetic parameter that represents the excess Gibbs free energy of mixing. The β_M parameter can be determined from experimental values of cmc_M using the following expressions:

$$\beta_M = \frac{\ln\left(\frac{\alpha_i\, cmc_M}{X_i\, cmc_i}\right)}{X_j^2} = \frac{\ln\left(\frac{\alpha_j\, cmc_M}{X_j\, cmc_j}\right)}{X_i^2} \tag{7}$$

The micellar composition X_i and the activity coefficients γ_i can be obtained from β_M by numerical solving the system formed by Eqs. 2–5. The β_M quantitatively captures the extent of non-ideality. The larger the negative values of β_M, the stronger the attractive interactions between the two different surfactants molecules. Repulsive interactions yield a positive β_M value, whereas $\beta_M = 0$ indicates an ideal mixture.

Motomura's Model (20). This model is an attempt to overcome the limitations of Rubingh's model and improve the predictions of the phase separation model. Basically, it is a thermodynamic method which considers the micelles as a macroscopic bulk phase, the thermodynamic quantities associated with the mixed micelle formation process being expressed as a function of the excess thermodynamic quantities. For a mixed system constituted by two surfactants, 1 and 2, which dissociated into ν_1 ($\nu_{1,a}$ and $\nu_{1,c}$) and ν_2 ($\nu_{2,b}$ and $\nu_{2,d}$) ions, respectively, the micellar composition is determined from the experimental values of the monomeric composition and the cmc_M, by the expression:

$$\overline{X}_2^{mic} = \overline{\alpha}_2 - \left(\frac{\overline{\alpha}_1\overline{\alpha}_2}{\overline{cmc}_M}\right)\left(\frac{\partial \overline{cmc}_M}{\partial \overline{\alpha}_2}\right)_{T,P}\left[1 - \frac{\delta_d^c \nu_{1,c}\nu_{2,d}}{\nu_{1,c}\nu_2\overline{\alpha}_1 + \nu_{2,d}\nu_1\overline{\alpha}_2}\right] \tag{8}$$

where

$$\overline{\alpha}_i = \frac{\nu_i\alpha_i}{\sum \nu_i\alpha_i}\ (i = 1, 2) \tag{9}$$

$$(i = 1, 2) \tag{10}$$

$$\overline{cmc}_M = cmc_M \sum \nu_i\alpha_i\ (i = 1, 2) \tag{11}$$

The Kroenecker delta, δ_d^c, is 1 for c = d and 0 for c ≠ d.

Results and Discussion

Critical Aggregation Concentration

The critical aggregation concentration (*cac*) is the most important parameter in investigations that concern the self-assemble of amphiphile type molecules. For surfactants mixtures, the determination of *cac* has an added interest, as discussed in the following. This is because some properties of mixed surfactant systems, such as the micellar phase composition cannot be measured directly but must be estimated using the proper mixing thermodynamic models and these models are based on the knowledge of *cac* over the whole range of compositions.

Fluorescence experiments were carried out to determine the *cac* values of mixed systems. Nevertheless, the critical aggregation concentration determination is very difficult due to the slow change, which is characteristic of successive stepwise association of NaDHC (9, 10). Therefore, to corroborate the obtained values other techniques (such as conductivity and surface tension) were necessary.

Pyrene is a polarity-sensitive probe (21) and its vibronic band intensities (I) in fluorescence yields information on *cac* and on the micellar structure (22–24). As Kalyanasundaram and Thomas (25) proved that the characteristic dependence of the fluorescence vibrational fine structure of pyrene could be used to determine the critical micelle concentration (cmc) of a surfactant solution; the so-called pyrene I_1/I_3 ratio method has become one of the most popular procedures for the determination of this important parameter for both pure and mixed micellar systems (26). This method is regarded as an invasive technique but since the pyrene concentration is very low compared to the surfactant concentration (which is at least a thousand times higher) it can be assumed that the probe effect was negligible on the micellization process.

As an example of the *cac* determination, Fig. 1 shows the variation of I_1/I_3 ratio of pyrene as a function of total surfactant concentration (C_T) just with the experimental surface tension (σ) isotherm for the $\alpha_{NaDHC} = 0.4$ system. The results show that the polarity of the environment around the pyrene molecules decreases with surfactant concentration increase. In other words, pyrene is solubilized into aggregates. However, the plot does not show (around *cac*) the typical sigmoidal decrease and the inflection point that can be used to estimated de *cac* (27). This fact has been explained in terms of pyrene partition between aggregates and bulk phase. In our particular case (low *cac* values), the volume of the hydrophobic pseudophase is not voluminous enough and pyrene partitions between this phases and bulk provide an average value of the pyrene I_1/I_3 ratio index corresponding to a more polar environment. In such conditions, the *cac* values can be obtained from the interception of the rapidly varying part and the nearly horizontal part at high concentration of the pyrene I_1/I_3 ratio plots (28). There were two clear transition points at the pyrene I_1/I_3 ratio vs C_T plot: (i) a sharp decrease that can be assumed as the beginning of aggregation (cac_1) and (ii) a less pronounced change that was assigned to a variation in aggregates' structure (cac_2). Two inflection points at similar concentrations were found from the analysis of σ vs. C_T curve.

The *cac* values can also be determined by the intersection of two straight lines above and below the inflection point of specific conductivity (κ) versus total surfactant concentration (C_T) plots. However for the tested systems, the κ vs. C_T curves show an increasingly weaker change in slopes before and after aggregation. To perform a better analysis of conductivity data $\Delta\kappa = \kappa - \kappa_{extrapolated}$ vs. C_T method was used (29). The $\kappa_{extrapolated}$ values were found by extrapolation of pre-cmc specific conductivity data by fitting them to least-squares straight line. This method magnifies the slope difference between pre- and post cmc data. Fig. 2, shows the Δκ vs C_T for the $\alpha_{NaDHC} = 0.4$ system, an inflection point can be seen at $C_T = 1.25 \times 10^{-4}$ mol dm^{-3} which much up with the obtained value of cac_1 from I_1/I_3 vs C_T and σ vs. C_T plots. Critical aggregation concentrations of all tested systems were determined in the same way; the results are summarized in Table 1.

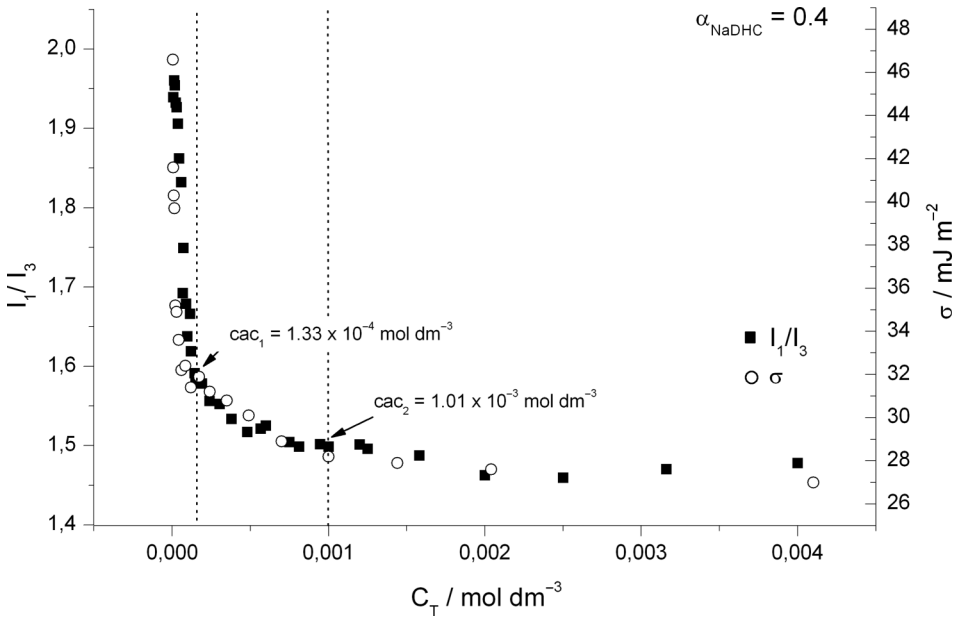

Fig. 1. Fluorescence intensities ratios of the first and third vibronic pick of Pyrene emission spectra (I_1/I_3) as a function of total surfactant concentration (C_T) just with the experimental surface tension (σ) isotherm for the $\alpha_{NaDHC} = 0.4$ system.

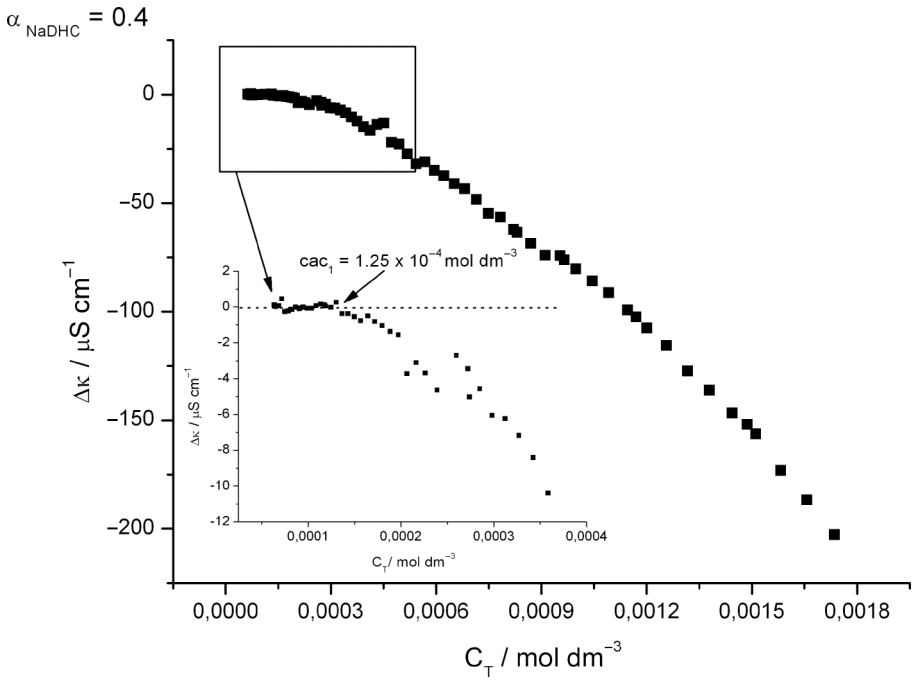

Fig. 2. $\Delta\kappa = \kappa - \kappa_{extrapolated}$ vs. C_T for the $\alpha_{NaDHC} = 0.4$ system.

Study of Aggregates Size and Structural Transitions

Taking into account that NaDHC molecules form micelles (9, 10) and DDAB molecules form vesicles at higher concentrations (30, 31), we presumed that the *cac$_1$* corresponded to micelle formation and *cac$_2$* to a structural aggregate transformation (probably vesicles). The characterization of aggregates' size and structure occurring in all mixed systems at $C_T \geq cac_1$ was further carried out by dynamic light scattering, ζ-potential and TEM imaging.

Figure 3 shows the transmission electron microphotographs (TEM) of $\alpha_{NaDHC} = 0$, 0.2, 0.4, 0.6 and 0.8 mixed system at different concentrations. The concentration range studied in this work corresponded to a very dilute DDAB-water phase diagram region (0.4–6mM). So according by to our findings at $C_T =$ 0.4 mM very small aggregates such as micelles would exist, while at higher concentrations ($C_T = 6$ mM) spheroid droplet-like aggregates of about 17–20 nm appear. Evidently, they are too large to be micellar aggregates; it is supposed that they probably

Table 1. I_1/I_2 ratio values at cac_1 (*) and cac_2 (§) for each system.

α_{NaDHC}	cac_1 /mM	I_1/I_2*	cac_2 /mM	I_1/I_2§
0	0.124	1.50	1.161	1.37
0.1	0.106	1.61	1.173	1.46
0.2	0.087	1.59	0.471	1.53
0.3	0.138	1.62	0.422	1.49
0.4	0.131	1.58	1.010	1.50
0.5	0.111	1.56	1.472	1.47
0.6	0.149	1.58	1.423	1.47
0.7	0.138	1.63	0.428	1.51
0.8	0.159	1.58	0.583	1.52
0.9	0.364	1.53	–	–
1	22.80	–	–	–

consist of a kind of vesicle. Marques et al. (31) obtained similar results.

The $\alpha_{NaDHC} = 0.2$ mixed system at low concentration (C_T = 0.4 mM) shows that the incorporation of bile salt molecules into small aggregates do not alter their behavior. At higher concentrations (C_T = 8 mM) small nanodroplets previously noted in pure DDAB system and multilamellar vesicles (onions domains) of 42–136 nm can be seen. Notably, differences are seen with the increment of NaDHC proportion ($\alpha_{NaDHC} = 0.4$). Here, at very low concentrations (C_T = 0.4 mM) micellar aggregates coexist with small vesicles (20 nm). An increment of surfactant concentration provokes the disappearance of nanodroplets and the formation of multi-lamellar vesicles. For the $\alpha_{NaDHC} = 0.6$ system, at C_T = 0.4 mM, micellar aggregates and small vesicles (20 nm) are observed; nevertheless at higher concentrations (C_T = 10 mM) only vesicles of about 200 nm appear.

Vesicles disappear at low concentration (C_T = 0.4 mM) for the $\alpha_{NaDHC} = 0.8$ mixture. However, small spherical droplet-like aggregates (260 nm) exist at C_T = 8 mM. Pure NaDHC systems form very small aggregates even at higher surfactant concentrations (0.1 M) (9, 10).

In this study we made DLS measurements (Fig. 4) to investigate the effect of NaDHC on the apparent size and polydispersity of DDAB vesicles in water. The diameter measured by DLS cannot be directly compared to that measured on TEM pictures because the latter method gives only a snapshot of a specimen, whereas DLS gives an average measurement of the bulk sample. Nevertheless, the obtained values were comparable.

At all tested total surfactant concentrations (C_T = 10; 16 and 25 mM), the hydrodynamic diameter first decreases and then increases with the augment of α_{NaDHC}. The minimum vesicle size appears at $\alpha_{NaDHC} = 0.3$. This can be explained from the view point of the ion-complex curvature. The anionic and cationic surfactants can form ion complexes because of electrostatic interactions. At low NaDHC, the generated ion-complex has a high curvature and the vesicles form with a small diameter. When more bile salt type molecules penetrate into the bilayer the curvature of the ion complex gets larger and the vesicles become smaller. At $\alpha_{NaDHC} = 0.3$ a surfactant recombination was supposed to occur with the further penetration of NaDHC. In such conditions, the ion complex has smaller curvature and the vesicle size becomes larger. The vesicle diameter augments from 200 to 500 nm and the polydispersity (P) is strongly dependent of C_T and α_{NaDHC}. Polydispersity is at maximum level at high C_T and DDAB bilayer content, but decreases with the increment of α_{NaDHC} with the increment of vesicle size. The increment of the total surfactant concentration can promote vesicle growth. Generally, two or more distributions peaks are observed in most spectra that show a much wider size distribution.

The mechanism for the formation of lamellar vesicles is complex due to the interplay of different types of interactions. The hydration theory and related water structuring effects can explain it in a simply manner. The size of the vesicles as well as the presence of large, fused vesicles is dependent on the nature of counterions of both components of the catanionic system. The effect of various ions on the formation of vesicles will depend on the manner in which these ions alter the area per molecule at the interface (32). According to Isrealachvili (7, 8), the formation of vesicles is favored when the packing parameter is close to one. This is mainly due to the decrease of the surface area occupied by the surfactant headgroups. As the surfactant ions and co-ions occupy the surface regions of the aggregates, they can effectively compete with the headgroups for water and that consequently the headgroups are less and less hydrated with increasing concentration of ions. The effects of the nature and type of ion depend on their cosmotropic or chaotropic nature (33). Due to the difference in surface charge density and, hence, the hydration of chaotropes and cosmotropes, chaotropes will form direct ion pairs with other chaotropes, and cosmotropes will interact more favorably with other cosmotropes (33, 34). Following Collins concept (35), chaotropes can form direct ions pairs with other chaotropes, much as cosmotropes with other cosmotropes, but chaotropes do not come into close contact with cosmotropes. Thus, it was concluded that oppositely charged ions in free solution spontaneously form inner sphere ion pairs only when they have equal water affinities. Dehydrocholate ion (DHC^-) behaves as a water-structure breaker (chaotrope). The large size and the stiffness of the steroid backbone and the presence of the polar groups in different part of the molecule hindered the formation of a structured water cage surrounding the surfactant molecule and favored the destruction of the "water icebergs" (36). In agreement with Collins' concept (35) the interaction of DHC^- (chaotrope) ion with DDA^+ (chaotrope) eliminated the H-bond formation between water and carboxylate and carbonyl

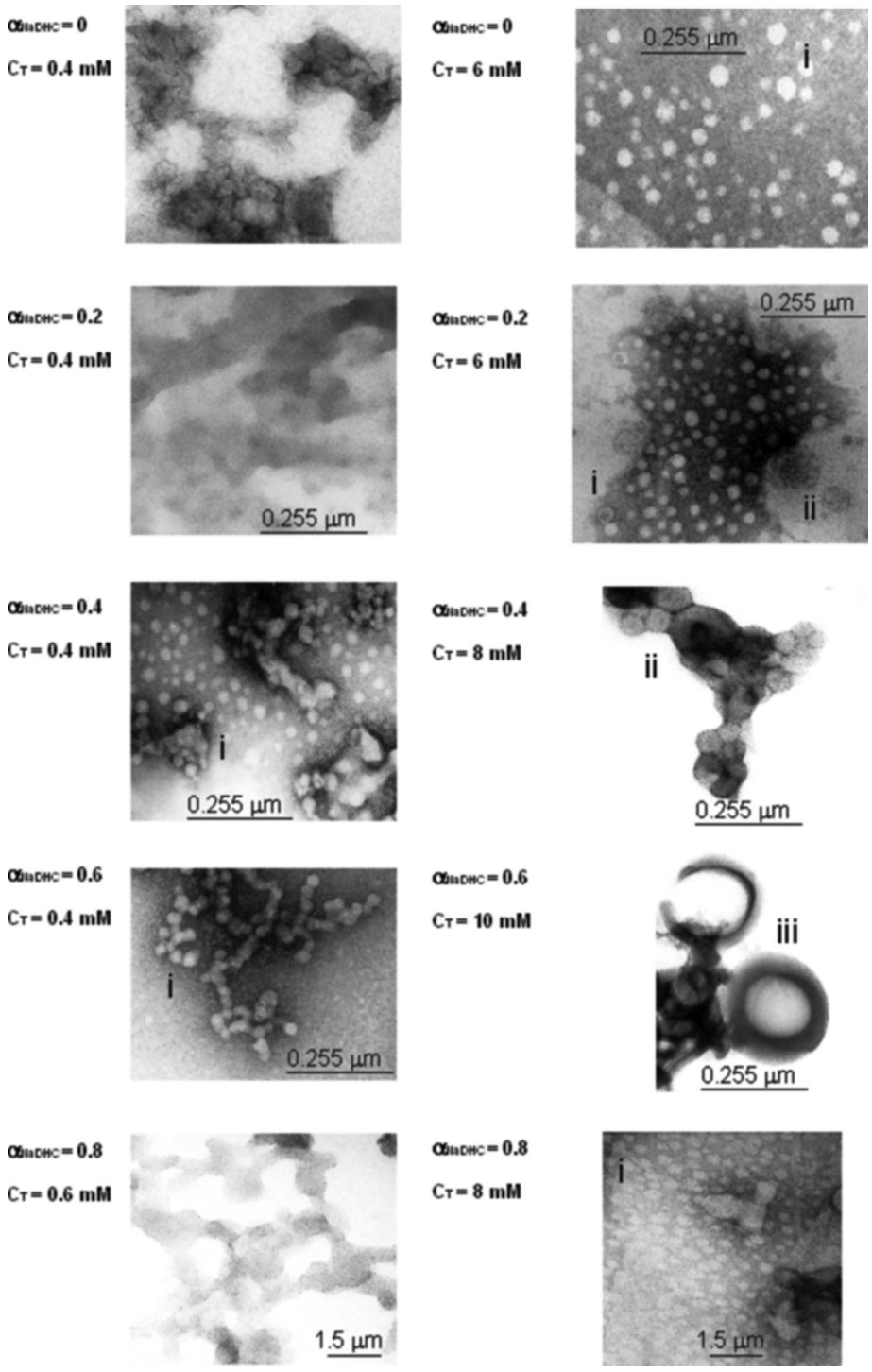

Fig. 3. Transmission electron microphotographs of $\alpha_{NaDHC} = 0$, 0.2, 0.4, 0.6 and 0.8 mixed system at different concentrations. (i) spheroid droplet-like aggregates; (ii) multilamellar vesicles (onions domains); (iii) vesicles.

groups of bile acid molecule. Thus, this ion pair or dipole would be much less hydrated than separate ions and headgroups. This smaller hydration was reflected in reduction of effective headgroups areas resulting in a higher packing parameters and the presence of larger structures in mixed systems compared with pure DDAB and NaDHC aggregates. Furthermore, the presence of the cosmotrope counterion Na^+ promoted the compression of the electrical bilayer of both molecules in mixed system and, consequently, the formation of bilayer and multi-lamellar type structures.

Figure 5 shows the ζ-potential of the mixed vesicles at different total surfactant concentration as a function of α_{NaDHC} at the temperature of 25°C. In calculating the ζ-potential of a small particle, the deformation of the applied field by the

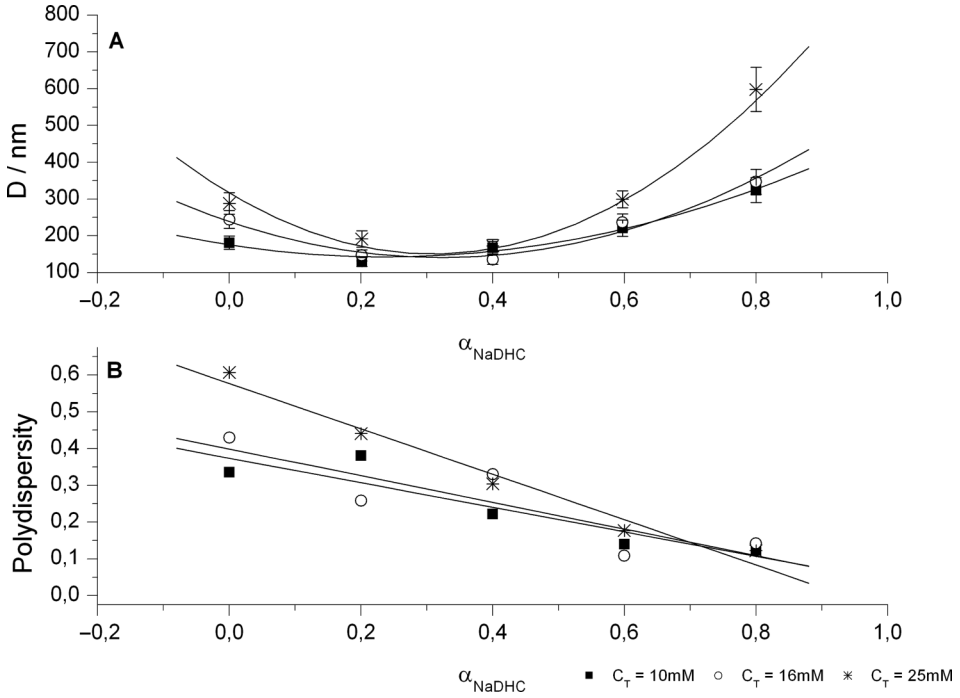

Fig. 4. Hydrodynamic radius (D) and Polydispersity variation as a function of α_{NaDHC} for different total surfactant concentrations (C_T).

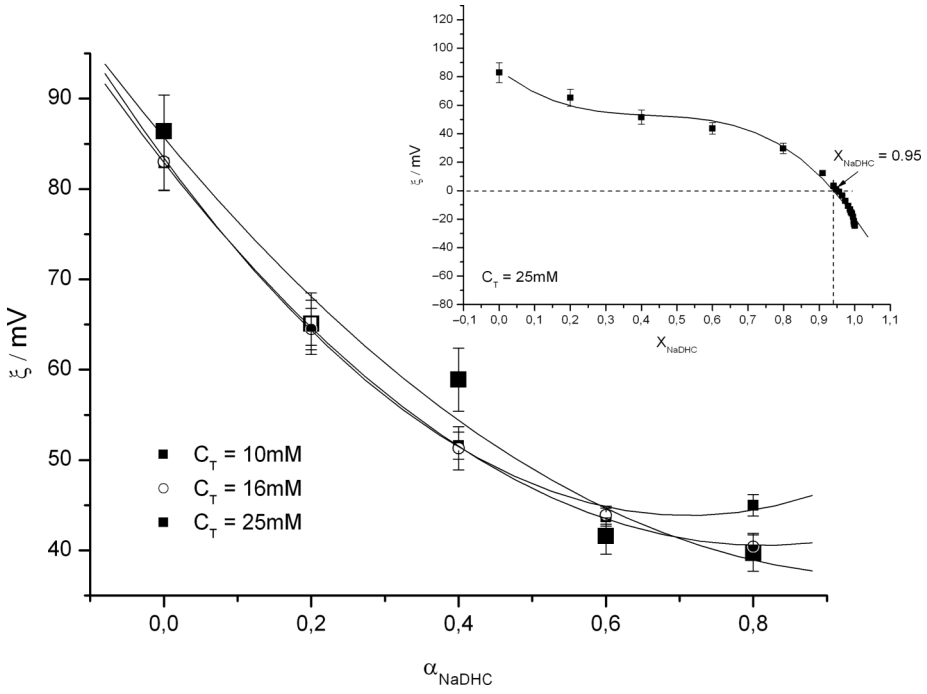

Fig. 5. ζ-potential of the mixed vesicles at different total surfactant concentration as a function of α_{NaDHC} at the temperature of 25°C.

presence of the particle in its neighborhood can be neglected. It may also be assumed that the electrophoretic retardation does not affect the particle to any great extent, and the only retarding force on the particle is the viscous drag from the water.

The vesicles ζ-potential was not appreciably affected by the increment of total surfactant concentration. The incorporation of NaDHC molecules into the bilayer do not change the positive signal of the vesicles ζ-potential, nevertheless a diminution of it absolute values can be appreciated confirming the electrostatic interaction between NaDHC and DDAB. At $\alpha_{NaDHC} = 0.95$, the sign of the aggregates ζ-potential changed from positive to negative (Fig. 5 insert). In such a condition, we were in the presence of micellar aggregates instead of vesicles.

The first and third vibronic peaks intensity ratio for pyrene fluorescence (I_1/I_3) was used for the evaluation of aggregates' micropolarity (37, 38). For low I_1/I_3 values, the microenvironment of the solubilized pyrene is non-polar or hydrophobic as in hydrocarbon solvents. Then, the values of I_1/I_3 ratio at cac_1 and cac_2 for each system (Table 1) were used as a first approximation to study the aggregates polarity.

The measured I_1/I_3 ratio for pyrene in water, ethanol, and C_6H_{14} were 1.91; 1.40, and 0.66, respectively (similar to those observed in literature (37, 39). The I_1/I_3 ratio values reported in Table 1 for all mixed systems were superior to 1.37, so we ended that fluorescence probe was placed in a highly polar microenvironment. Going on again to Table 1, it can be noticed a slightly decrease of I_1/I_3 ratio as the aggregates go from micelles to vesicles. The changes of aggregates' shape favored the pyrene dissolution in their hydrophobic interior.

All mixed systems presented a micropolarity higher than that of pure DDAB aggregates and such fact was more evident as the aggregates size augment. Such fact suggests that the presence of bile salt alter notably the aggregates' palisade layer (where pyrene solubilization occurs). Such a change, even minor, of pyrene solubilization site would cause a change of micropolary. The intercalation of cholesteric ring among hydrocarbon tails may bring pyrene slightly closer to micelle surface with the consequent augment of micro polarity value; similar results were found in literature (38).

Micellar Surfactant Interactions

The dependence of the cac_1 (CMC) on the surfactant mixture composition is shown in Fig. 6. The obtained cac_1 values for the pure DDAB system were consistent with literature ($\approx$ 0.1 mM) (30). The micelle composition was computed with Rubingh and Motomura's models (19, 20) and plotted in Fig. 7 together with the ideal behavior. The CMC values for different DDAB-NaDHC mixtures show attractive interactions at all compositions. Figure 7 shows that micellar aggregates were comprised by about 15–30% mol of NaDHC and such value was almost independent of bulk composition. In a similar system Marques et al. (31) determined that in the dilute region, DDAB vesicles are able to incorporate about 20 mol% of bile salt. This composition is preferential and it interpretation is similar to a saturation limit. In consideration of our obtained results, we can suppose that such fact is also applicable to NaDHC-DDAB aggregates.

To gain quantitative understanding of the mixing process is worth applying the regular solution theory to obtain $\beta_{M,}$ the dimensionless intramicellar interaction parameter. The computed β_M values are negative and about constant at all compositions ($\beta_M \approx -7.77$ kT). Such high negative is a typical value for catanionic mixtures (40) and is related to attractive interactions. Such interactions were previously inferred from the analysis of Fig. 6. Rosen et al. have defined the synergism in mixed micelles when the cmc of the mixture is smaller than the cmc's of individual pure surfactants and two conditions were established to achieve the synergism (41, 42): (i) β_M must be negative (two surfactants must attract each other in the mixed micelle) and (ii) $|\beta_M| > |\ln(cmc_1/cmc_2)|$ (this attraction must be greater than the differences between the natural logs in their cmc values). When these considerations are taken into account, the results indicate that for all compositions our system presents a large synergism.

The activity coefficients of both surfactants in mixed micelles (γ) are shown in Fig. 8 as a function of the square root of micelle composition. At high DDAB micellar content γ_{DDAB} remained near the ideal value ($\approx$1). This infers that the mixed aggregate neighborhoods for these surfactant molecules are not very different from those in pure DDAB micelles. This behavior is typical of the activity coefficient in the solvent, since in the phase separation model $\gamma = 1$ for the pure component.

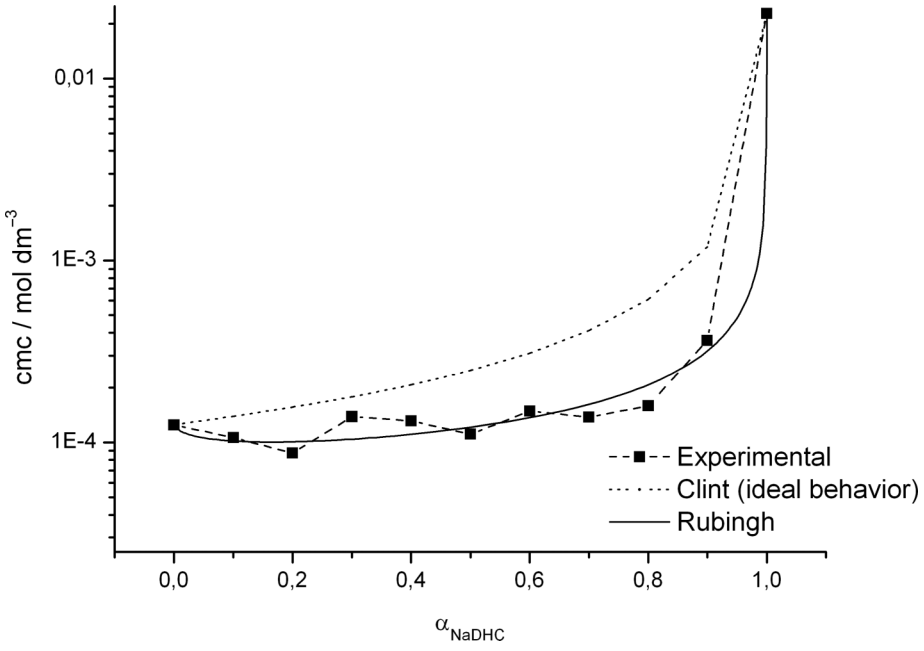

Fig. 6. Critical micelle concentration (CMC) dependence on the molar fraction of NaDHC (α_{NaDHC}) in the mixed surfactant system.

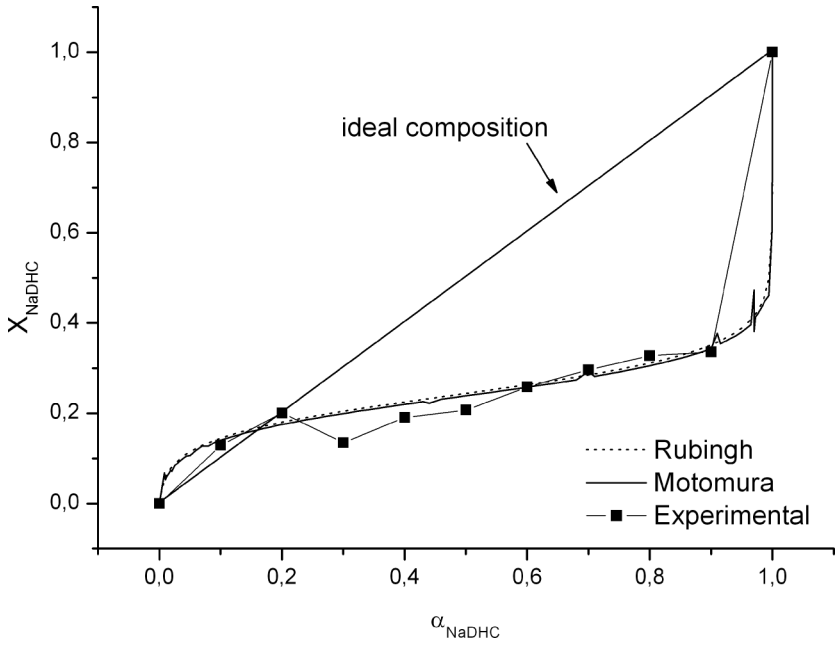

Fig. 7. Variation of mole fraction of NaDHC in mixed micelles (X_{NaDHC}) versus surfactant mixture composition (α_{NaDHC}), computed with Rubingh and Motomura treatments.

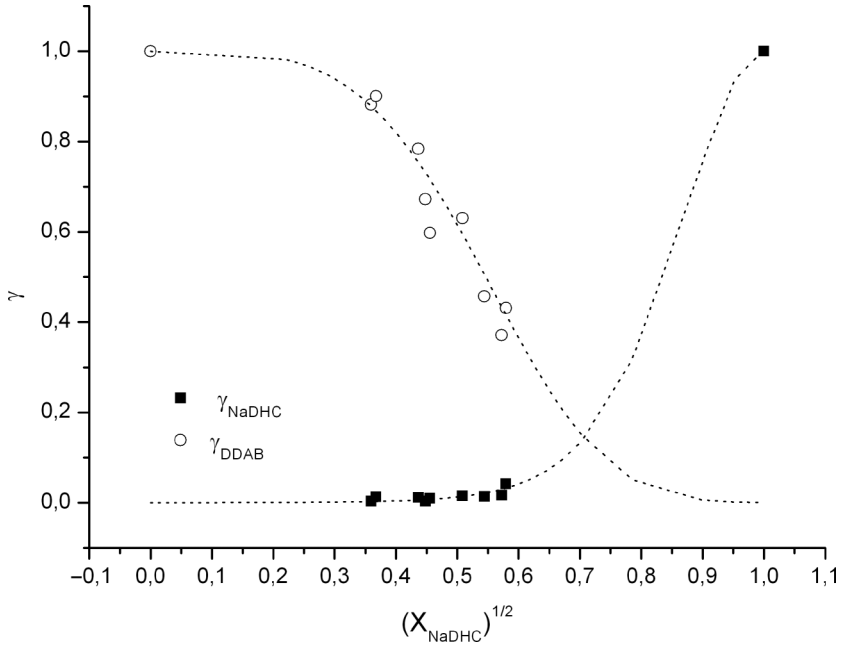

Fig. 8. Activity coefficient (γ) of NaDHC and DDAB in micelles vs. the square root of the micelle composition $(\alpha_{NaDHC})^{1/2}$ obtained from the regular solution theory applied to mixed micellization. Dashed lines represent the theoretical adjust based on Rubingh model.

As the micellar content of NaDHC increased, γ_{DDAB} decreased noticing that the intercalation of bile salt molecule changes the surfactant microenvironment. On the other hand, γ_{NaDHC} is very lower than unity showing a high attraction of such surfactant to integrate the mixed micelles, which are majority composed by DDAB. The gradual inclusion of NaDHC molecules inside DDAB micelles causes a structural accommodation of steroidal rings among DDAB hydrocarbons tails favoring the attraction interactions between surfactants. The $\gamma_{NaDHC} << 1$ showed that the microenvironment of NaDHC molecules in the mixed aggregates was very different from that in pure NaDHC micelles that is the bile salt derivative surroundings are composed by DDAB. NaDHC acted as a highly soluble solute. The intercalation of flexible hydrocarbon tail chains of DDAB among the rigid cholesteric structures must minimize the hydrocarbon-water contact of bile salt molecules in comparison with pure dehydrocholate micelles, but probably did not affect significantly that between DDAB

chains and water. Such behavior was evidenced in a previous work (43, 44).

Conclusion

The phase behavior for the very dilute DDAB-NaDHC–water system was investigated at 25°C. Comparisons between experimental and calculated values showed the suitability of the regular theory to predict CMC values for the tested systems. The interaction between both amphiphiles inside aggregates is not ideal showing a large synergism. Such fact is reflected by the activity coefficients values. The aggregates are mainly composed by DDAB (18–30% mol NaDHC) regardless of the NaDHC solution molar fraction; these molecules act as a good solvent of bile salt type molecule. Nevertheless, the gradual inclusion of NaDHC molecules leads to structural transformations. The incorporation of NaDHC into DDAB bilayers had two effects: (i) the interaction of DHC^- and DDA^+ (chaotropes) ions form an ion pair or dipole that would be much less hydrated than separate ions headgroups, this smaller hydration is reflected in the reduction of effective headgroups areas; and (ii) in contrast, the intercalation of the rigid ring-based of bile salts between DDAB chains also causes an increment of chain repulsion due to steric effect. Accordingly, the $X_{NaDHC} = 0.2$ and 0.4 systems experimented a micellar → spheroid droplet-like aggregate → multilamellar vesicle transitions. For the $X_{NaDHC} = 0.6$ and 0.8 mixed system, the droplet-like aggregates transformed into unilamellar vesicles of about 200–500nm diameter. Finally, the mixed $X_{NaDHC} = 0.9$ system showed only a micellar aggregates.

Aggregates micropolarity was also studied. All mixed systems present a higher micropolarity than that of pure DDAB aggregates and such fact is more evident as the aggregates size augment. Such facts confirm that the presence of bile salt alters notably the aggregates' palisade layer (where pyrene solubilization occurs).

Acknowledgments

The authors acknowledge the financial support from the Universidad Nacional del Sur, Agencia Nacional de Promoción Científica y Tecnológica (ANPCyT) and Concejo Nacional de Investigaciones Científicas y Técnicas de la República Argentina (CONICET). PM is an adjunct researcher of (CONICET). M.D. Fernández-Leyes and C. Luengo have a fellowship from the CONICET. The authors want to especially thank Dr. Marcelo Avena (Departamento de Química, Universidad Nacional del Sur, INQUISUR-CONICET. 8000 Bahía Blanca, Argentina) for his collaboration.

References

1. Ramos Cabrer, P., Alvarez-Parrilla, E., Al-Soufi, W., Meijide, F., Rodríguez Núñez, E., and Vázquez Tato, J. (2003) Complexation of bile salts by natural cyclodextrins. *Supramolecul. Chem.*, 15(1):33–43.
2. Fernadez-Leyes, M., Messina, P., and Schulz, P. (2007) Aqueous sodium dehydrocholate–sodium deoxycholate mixtures at low concentration. *J. Colloid Interf. Sci.*, 314(2):659–664.
3. Thongngam, M., and McClements, D.J. (2005) Isothermal titration calorimetry study of the interactions between chitosan and a bile salt (sodium taurocholate). *Food Hydrocolloid*, 19(5):813–819.
4. Singh, T.S., and Mitra, S. (2009) Fluorescence properties of trans-ethyl-p-(dimethylamino) cinnamate in presence of bile acid host. *J. Photochem. Photobiol. B*, 96(3):193–200.
5. Youssry, M., Coppola, L., Marques, E.F., and Nicotera, I. (2008) Unravelling micellar structure and dynamics in an unusually extensive DDAB/bile salt catanionic solution by rheology and NMR-diffusometry. *J. Colloid Interface Sci.*, 324(1–2):192–198.
6. Bhat, S., Leikin-Gobbi, D., Konikoff, F.M., and Maitra, U. (2006) Use of novel cationic bile salts in cholesterol crystallization and solubilization in vitro. *Biochim. Biophys. Acta*, 1760(10):1489–1496.
7. Israelachvili, J.N, Mitchell, D.J., and Ninham, B.W. (1976) Amphiphiles into micelles and bilayers. *J. Chem. Soc. Faraday Trans.*, 2(72):1525–1568.
8. Sjöbom, M.B., Marques, E.F., Edlund, H., and Khan, A. (2005) Phase equilibria of the mixed didodecyldimethylammonium bromide-sodium taurodeoxycholate-water system with a large solution region. *Colloid Surfaces A*, 269:87–98.
9. Messina, P., Morini, M.A., Schulz, P.C., and Ferrat, G. (2002) The aggregation of sodium dehydrocholate in water. *Colloid Polym. Sci.*, 280:328–335.
10. Schulz, P.C., Messina, P., Morini, M.A., and Vuano, B. (2002) Potentiometric studies on sodium dehydrocholate micelles. *Colloid Polym. Sci.*, 280:1104–1109.
11. Marques, E.F., Khan, A., and Lindman, B. (2002). A calorimetric study of the gel-to-liquid crystal transition in catanionic surfactant vesicles. *Thermochim. Acta.*, 394 31–37.
12. Barreleiro, P.C.A., Olofsson, G., Brown, W., Edwards, K., Onsái, N., and Feitosa, E. (2002) interaction of octaethylene glycol n-dodecyl monoether with dioctadecyldimethylammonium bromide and chloride vesicles. *Langmuir*, 18:1024–1029.
13. Kunitake, T., and Okahata, Y. (1980) Formation of the stable bilayer assemblies in dilute aqueous solution from ammonium amphiphiles with the diphenylazomethine segment. *J. Am. Chem. Soc.*, 102:549–553.
14. Matteini, P., Brustolon, M., Turro, N.J., Jocusch, S., and Tomalia, D.A. (1998) Characterization of starburst dendrimers and vesicle solutions and their interactions by CW- and pulsed-EPR, TEM, and dynamic light scattering. *J. Phys. Chem. B*, 102:6029–6039.
15. Henry, D.C. (1931) The cataphoresis of suspended particles. Proc. Roy. Soc. London Ser. A, 133:106–129.
16. Holland, P.M., and Rubingh, D.N. (1992) *Mixed Surfactant Systems*; American Chemical Society: Washington, D.C.
17. Clint, J.H. (1975) Micellization of mixed nonionic surface active agents. *J. Chem. Soc. Faraday Trans.*, 1 (71):1327–1334.
18. Junquera, E., and Aicart, E. (2002) Mixed micellization of dodecylethyldimethylammonium bromide and dodecyltrimethylammonium bromide in aqueous solution. *Langmuir*, 18:9250–9258.
19. Holland, P.M., and Rubingh, D.N. (1983) Nonideal multicomponent mixed micelle model. *J. Phys. Chem.*, 87:1984–1990.
20. Motomura, K., Yamanaka, M., and Aratono, M. (1984) Thermodynamic consideration of the mixed micelle of surfactants. *Colloid. Polym. Sci.*, 262(12):948–955.
21. Nakajima, A. (1976) Fluorescence spectra of pyrene in chlorinated aromatic solvents. *J. Luminescence*, 11(5–6):429–432.
22. Azum, N., Naqvi, A.Z., Akram, M., and -ud-Din, K. (2008) Studies of mixed micelle formation between cationic gemini and cationic conventional surfactants. *J. Colloid Interface Sci.*, 328(2):429–435.
23. Chaudhuri, A., Haldar, S., and Chattopadhyay, A. (2009) Organization and dynamics in micellar structural transition monitored by pyrene fluorescence. *Biochem. Biophys. Res. Comm.*, 390(3):728–732.
24. Sadoqi, M., Lau-Cam, C.A., and Wu S.H. (2009) Investigation of the micellar properties of the tocopheryl polyethylene glycol succinate surfactants TPGS 400 and TPGS 1000 by steady state fluorometry. *J. Colloid Interface Sci.*, 333(2):585–589.
25. Kalyanasundaran, K., and Thomas, J.K. (1977) Environmental effects on vibronic band intensities in pyrene monomer fluorescence and

their application in studies of micellar systems. *J. Am. Chem. Soc.*, 99(7):2039–2044.
26. Aguiar, J., Carpena, P., Molina-Bolivar, J.A., and Carnero-Ruiz, C. (2003) On the determination of the critical micelle concentration by the pyrene 1:3 ratio method. *J. Colloid Interface Sci.*, 258(1):116–122, and references therein.
27. Zana, R., Lévy, H., and Kwetkat, K. (1998) Mixed micellization of dimeric (Gemini) surfactants and conventional surfactants. I. Mixtures of an anionic dimeric surfactant and of the nonionic surfactants $C_{12}E_5$and $C_{12}E_8$. *J. Colloid Interface Sci.*, 197(2):370–376.
28. Frindi, M., Michels, B., and Zana, R. (1992) Ultrasonic absorption studies of surfactant exchange between micelles and bulk phase in aqueous micellar solutions of nonionic surfactants with a short alkyl chain. 3. Surfactants with a sugar head group. *J. Phys. Chem.*, 96(20):8137–8141.
29. Miura, M., and Kodama, M. (1972) The second CMC of the aqueous solution of sodium dodecyl sulfate. I. Conductivity. *Bull. Chem. Soc. Jpn.*, 45(2):428–431.
30. Kodama, T., Ohta, A., Toda, K., Katada, T., Asakawa, T., and Miyagishi, S. (2006) Fluorescence-probe study of vesicle and micelle formations in a binary cationic surfactants system. *Colloid Surfaces A*, 277(1–3):20–26.
31. Marques, F.E., and Khan, A. (2002) Effect of a bile salt on the aggregation behavior of a double-chained cationic surfactant – the cationic-rich dilute region of the didodecyldimethylammonium bromide-sodium taurodeoxycholate-water system. *Progr. Colloid Polym. Sci.*, 120:83–91, and references therein
32. Singh, K., Marangoni, D. G., Quinn, J.G., and Singer, R.D. (2009) Spontaneous vesicle formation with an ionic liquid amphiphile. *J. Colloid Interface Sci.*, 335:105–111.
33. Vlachy, N., Jagoda-Cwiklik, B., Vácha, R, Touraud, D., Jungwirth, P., and Kunz, W. (2009) Hofmeister series and specific interactions of charged headgroups with aqueous ions. *Adv. Colloid Interface Sci.*, 146:42–47.
34. Kunz, W., Henle, J., and Ninham, B.W. (2004) Zur Lehre von der Wirkung del Salze(about the science of the effect of salts): Franz Hofmeister's hystorical papers. *Curr. Opin. Colloid Interface Sci.*, 9(2004):19–37.
35. Collins, K.D. (2004) Ions from the Hofmeister series and osmolytes: Effects on proteins in solution and in the crystallization process. *Methods* 34:300–311.
36. Collins, K.D., Nielson, G.W, and Enderby, J.E. (2007) Ions in water: Characterizing the forces that control chemical processes and biological structure. *Biophys. Chem.*, 128:95–104.
37. Messina, P.V., Ruso, J.M., Prieto, G., Fernadez-Leyes, M., Schulz, P., and Sarmiento, F. (2010) Ca2+ and Mg2+ induced molecular interactions in a dehydrocholic acid: didodecyldimethylammonium bromide mixed monolayer. *Colloid Polymer Sci.* 288:449–459 and references therein.
38. Asakawa, T., Okada, T., Hayasaka, T., Kuwamoto, K., Ohta, A., and Miyagishi, S. (2006) The unusual micelle micropolarity of partially fluorinated gemini surfactants sensed by pyrene fluorescence. *Langmuir* 22(14):6053–6055.
39. Zana, R., and Lévy, H. (1997) alkanediyl-α, ω-bis(dimethylalkylammonium bromide). 7. fluorescence probing studies of micelle micropolarity and microviscosity. *Langmuir*, 13(21):5552–5557, and references therein.
40. Rodriguez, A., Junquera, E., del Burgo, Patricia, and Aicart, E. (2004) Conductometric and spectrofluorimetric characterization of the mixed micelles constituted by dodecyltrimethylammonium bromide and a tricyclic antidepressant drug in aqueous solution. *J. Colloid Interface Sci.*, 269:476–483.
41. Evans, H. C. (1956) Alkyl sulphates. Part I. Critical micelle concentrations of the sodium salts. *J. Chem Soc.*, 1:579–586.
42. Rosen, M.J. (1991) Synergism in mixtures containing zwitterionic surfactants. *Langmuir*, 7(5):885–888.
43. Hua, X.Y., and Rosen, M.J. (1982) Synergism in binary mixtures of surfactants : I. Theoretical analysis. *J. Colloid Interface Sci.*, 90(1):212–219.
44. Messina, P., Morini, M.A., and Schulz, P.C. (2003) Aqueous sodium oleate–sodium dehydrocholate mixtures at low concentration. *Colloid Polym. Sci.* 281:1082–1091.